Using chaos for remote sensing of laser radiation

Weng W. Chow[1,2] **and Sebastian Wieczorek**[3]

[1]*Sandia National Laboratories, Albuquerque, New Mexico 87185-1086, USA*
[2]*Physics Dept. and Institute of Quantum Studies, Texas A&M University, College Station, Texas 77843, USA*
[3]*Mathematics Research Institute, University of Exeter, Exeter EX4 4QF, UK*
wwchow@sandia.gov

Abstract: An idea is proposed for detecting a weak laser signal from a remote source in the presence of strong background noise. The scheme exploits dynamical nonlinearities arising from heterodyning signal and reference fields inside an active reference laser cavity. This paper shows that for certain reference laser configurations, the resulting bifurcations in the reference laser may be used as warning of irradiation by a laser source.

OCIS codes: (140.5960) Semiconductor lasers; (140.1540) Chaos; (280.3420) Laser sensors.

References and links

1. B. Krauskopf and D. Lenstra (Eds.), *Fundamental Issues of Nonlinear Laser Dynamics*, AIP Conference Proceedings, vol. 548, 2000.
2. D. M. Kane and K. A. Shore (Eds.), *Unlocking Dynamical Diversity: Optical Feedback Effects on Semiconductor Lasers*, (Wiley, 2005, pp. 147-183).
3. S. Wieczorek, B. Krauskopf, T.B. Simpson, and D. Lenstra, "The dynamical complexity of optically injected semiconductor lasers," Phys. Rep. **416**, 1–128 (20050.
4. G. Vemuri and R. Roy, "Super-regenerative laser receiver: Transient dynamics of a laser with an external signal," Phys. Rev. A **39**, 2539-2543 (1989).
5. I. Littler, S. Balle, K. Bergmann, G. Vemuri, and R. Roy, "Detection of weak signals via the decay of an unstable state: Initiation of an injection-seeded laser," Phys. Rev. A **41**, 4131-4134 (1990).
6. E. Lacot, R. Day, and F. Stoeckel, "Coherent laser detection by frequency-shifted optical feedback," Phys. Rev. A **64**, 043815-043825 (2001).
7. E. Lacot, O. Hugon, and F. Stoeckel, "Hopf amplification of frequency-shifted optical feedback," Phys. Rev. A **67**, 053806-053815 (2003).
8. M. B. Spencer and W. E. Lamb, Jr., "Laser with a Transmitting Mirror," Phys. Rev. A **5**, 884-892 (1972).
9. R. Lang, "Injection locking properties of a semiconductor laser," IEEE J. Quantum Electron. **18**, 976–983 (1982).
10. F. T. Arecchi, R. Meucci, G. Puccioni, and J. Tredicce, "Deterministic chaos in lasers with injected signal," Opt. Commun. **51**, 308-314 (1984).
11. T. B. Simpson, J.M. Liu, A. Gavrielides, V. Kovanis, and P. M. Alsing, "Period-doubling cascades and chaos in a semiconductor laser with optical injection," Phys. Rev. A **51**, 4181–4185 (1995).
12. T. Erneux, V. Kovanis, A. Gavrielides, and P. M. Alsing, "Mechanism for period-doubling bifurcation in a semiconductor laser subject to optical injection," Phys. Rev. A **53**, 4372–4380 (1996).
13. T. B. Simpson, "Mapping the nonlinear dynamics of a distributed feedback semiconductor laser subject to external optical injection," Opt. Commun. **215**, 135-151 (2003).
14. N. Shunk and K. Peterman, "Noise analysis of injection-locked semiconductor injection lasers," IEEE J. Quantum Electron. **22**, 642-650 (1986).
15. W. A. van der Graaf, A. M. Levine, and D. Lenstra, "Diode lasers locked to noisy injection," IEEE J. Quantum Electron. **33**, 434-442 (1997).
16. S. K. Hwang, J. B. Gao, and J. M. Liu, "Noise-induced chaos in an optically injected semiconductor laser model," Phys. Rev. E **61**, 5162-5170 (2000).
17. C. H. Henry, "Theory of the linewidth of semiconductor laser," IEEE J. Quantum Electron. **18**, 259–264 (1982).

#107230 - $15.00 USD Received 3 Mar 2009; revised 27 Mar 2009; accepted 6 Apr 2009; published 22 Apr 2009

18. G. Vemuri and R. Roy, "Effect of injected field statistics on transient dynamics of an injection seeded laser," Opt. Commun. **77**, 471-493 (1990).
19. E. Doedel, A. Champneys, T. Fairgrieve, Yu. Kuznetsov, B. Sandstede, and X. Wang, "AUTO 2000: Continuation and bifurcation software for ordinary differential equations," *http://sourceforge.net/projects/auto2000/*.
20. S. Valling, T. Fordell, and A. M. Lindberg, "Maps of the dynamics of an optically injected solid-state laser," Phys. Rev. A **72**, 033810–33818 (2005).

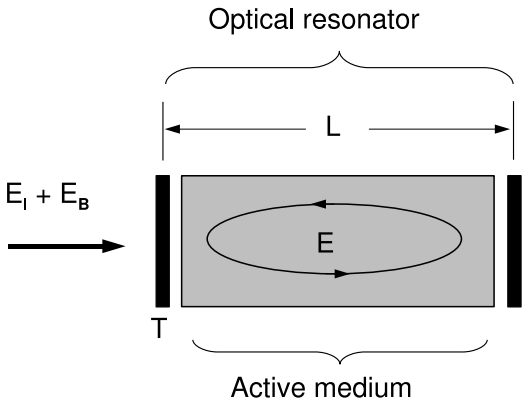

Fig. 1. Sketch of experimental setup showing the reference laser with intracavity electric field, E. The injected signal, consisting of coherent and incoherent contributions, E_I and E_B, respectively, mixes with the reference laser field after passing through a resonator mirror of transmission, T. The cavity length is L and the effects of the active medium is represented by a complex susceptibility.

1. Introduction

A challenging sensor problem involves the detection and discrimination of weak laser radiation from a strong incoherent background. Present attempts mainly involve classical approaches using spatial or temporal coherence. To achieve the necessary sensitivity, the engineering of these passive detection systems is demanding. This paper proposes an alternative, based on qualitative changes in dynamical behavior (bifurcations or instabilities) exhibited by a laser subjected to an external signal. Figure 1 is a sketch of the basic experimental setup. It is quite similar to heterodyne detection, with the important exception that the signal and reference beams are combined inside, instead of outside, the reference laser. With the mixing occurring inside an active cavity, the process becomes highly nonlinear, changing entirely the nature of the detection mechanism. In our scheme, the presence of external laser radiation is signaled by the crossing of bifurcation boundaries separating stable from chaotic operation.

Laser instabilities is an active research field. In particular, there is much focus on semiconductor lasers because of their rich dynamical behaviors. A free-running semiconductor laser is usually dynamically stable, capable only of damped relaxation oscillation. However, the situation changes when it is subjected to a stimulus, e.g., optical injection, external feedback or coupling to another laser. In these situations, a semiconductor laser may undergo a number of bifurcations leading to periodic, quasiperiodic or chaotic oscillations [1, 2, 3]. Most importantly, laser dynamical behavior for certain configurations can become extremely sensitive to the intensity and coherence of the injected field.

#107230 - $15.00 USD Received 3 Mar 2009; revised 27 Mar 2009; accepted 6 Apr 2009; published 22 Apr 2009

Table I: Input parameters for numerical simulations

Parameter	Variable	Value
Transparency carrier density	N_{tr}	$2\times10^{24}m^{-3}$
Differential gain	ξ	$10^{19}m^2$
Background refractive index	n_b	3.4
Linewidth enhancement factor	α	4
Confinement factor	Γ	0.05
Carrier decay rate	γ_N	10^9s^{-1}
Photon decay rate	γ_E	$10^{12}s^{-1}$
Laser wavelength	λ	$1\mu m$
Cavity length	L	$1\mu m$
Coupling mirror transmission	T	0.01

There already exist proposals exploiting optical nonlinearities for detecting weak coherent optical signals. Examples include using the sensitive dependence of laser switch-on time to injected field coherence [4, 5] and the strong enhancement of beating in intracavity laser fields to detect the presence of optical feedback [6, 7]. In our case, we use the bifurcation sensitivity of a semiconductor laser to external perturbation to produce sharp transitions between regular and complicated intensity oscillations. This paper examines whether these externally-induced instabilities and ensuing chaos may provide remote and instantaneous indication of the presence of coherent radiation even when masked by an incoherent background. The situation of coherent external perturbation has been much studied [8, 9, 10, 11, 12, 13, 3]. Not as well understood and important to our idea are noise effects, such as the influence of injected field fluctuations [14, 15, 16].

2. Theory

To investigate noise effects in injection locking, we use a rate equation model where laser behavior is described by a complex intracavity-field amplitude, E and total carrier density, N. The justification for reducing the complicated semiconductor laser device to just two system variables is based on the carrier relaxation rates being much faster than any temporal variations in laser field and total carrier population. This allows the active-medium polarization to adiabatically follow the field and population variations, with the carrier populations described by quasiequilibrium distributions. Then, semiclassical laser theory gives the following equations of motion, [9]

$$\frac{dE}{dt} = i2\pi\Delta E - \gamma_E E + \frac{c}{n_b}\Gamma\xi(N-N_{th})(1-i\alpha)E + F_L + \frac{c\sqrt{T}}{2n_bL}\left[E_I + E_B\right], \tag{1}$$

$$\frac{dN}{dt} = \Lambda - \gamma_N N - \frac{\varepsilon_0 n_b c}{\hbar\nu}\left[g_{th} + \xi(N-N_{th})\right]|E|^2, \tag{2}$$

where Δ is the detuning between injected and free-running laser central frequencies, Γ is the confinement factor, ξ is the differential gain at threshold carrier density, α is the linewidth enhancement factor, Λ is the pump rate, γ_E and γ_N are the photon and population decay rates, respectively, c is the speed of light in vacuum and n_b is the background refractive index. The threshold gain and carrier density in the free-running reference laser are given by $g_{th} = n_b\gamma_E(2c\Gamma)^{-1}$ and $N_{th} = N_{tr} + g_{th}\xi^{-1}$, where N_{tr} is the transparency carrier density. We

#107230 - $15.00 USD Received 3 Mar 2009; revised 27 Mar 2009; accepted 6 Apr 2009; published 22 Apr 2009

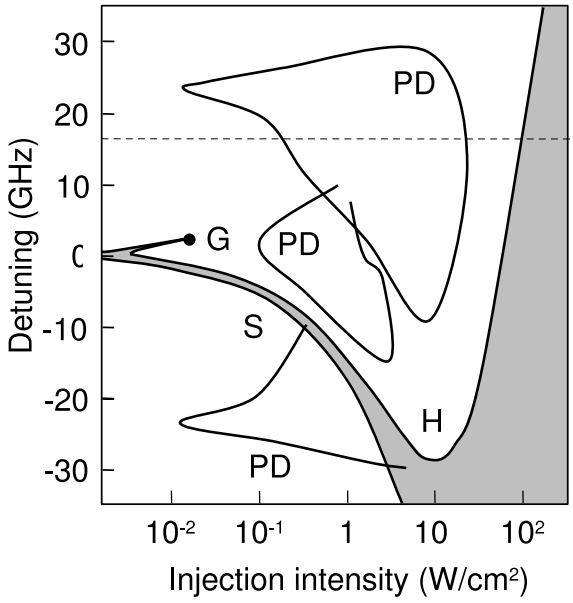

Fig. 2. Bifurcation diagram in plane of coherent injected intensity and frequency detuning for $\Lambda = 4$. The laser specification (Table 1) is typical for microcavity laser operating with a quantum-well gain medium. The dashed line indicates a one-dimensional bifurcation transition for $\Delta = 17$ GHz that is illustrated in Figs. 3-9.

account for the effect of reference laser noise from spontaneous emission and cavity optical-path length fluctuations by the complex random number function $F_L = F_L' + iF_L''$ with statistical properties given by

$$\langle F_L(t)\rangle = \langle F_L'(t)F_L''(t')\rangle = 0 \tag{3}$$

$$\langle F_L'(t)F_L'(t')\rangle = \langle F_L''(t)F_L''(t')\rangle = 2D_L\delta(t-t') \tag{4}$$

where for the case of only spontaneous emission noise, [17]

$$D_L = \frac{\hbar\nu}{\varepsilon_0\varepsilon_b}\beta\gamma_N N_{th}\delta(t-t') \tag{5}$$

ν is the lasing frequency and β is the fraction of spontaneous emission energy into the lasing mode. The noise leads to a reference laser linewidth (full-width at half maximum) of $\Delta\nu_L$. The injected fields, $E_a(t) = |E_a|\exp(-i\phi_a)$ where $a = I$ and B, are from the external laser signal and background noise, respectively. Assuming that the noise in these fields arises solely from phase fluctuation, we have

$$\frac{d\phi_a}{dt} = F_a(t) \tag{6}$$

where F_a is a random number function with

$$\langle F_a(t)F_a(t')\rangle = 2\pi\Delta\nu_a\delta(t-t') \tag{7}$$

and $\Delta\nu_a$, the spectral linewidth, is an input parameter. The injected field polarizations are assumed to be same as that of the reference laser. For unpolarized injected fields, E_a is the projection onto the reference laser polarization. There will be contributions in the orthogonal polarization, which typically sees less net gain. If this is not the case, mode competition may become

#107230 - $15.00 USD Received 3 Mar 2009; revised 27 Mar 2009; accepted 6 Apr 2009; published 22 Apr 2009

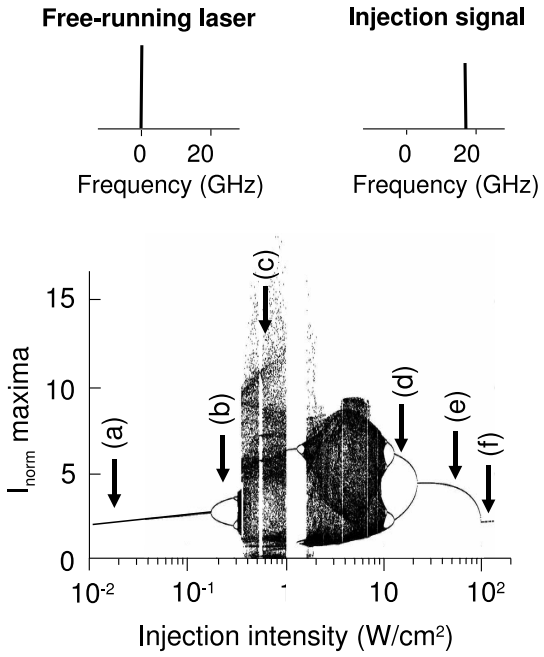

Fig. 3. Intensity maxima versus injected intensity for the noise-free case (see top sketch); $\Lambda = 4$ and $\Delta = 17$ GHz. The arrows indicate the injected intensities for the spectra in Fig. 4.

important, which may result in interesting dynamics. This multimode situation is beyond the scope of the present analysis.

2.1. Optical injection induced instabilities in the absence of noise

We begin by applying the model to describe a laser injected with a coherent signal and in the absence of noise. The purpose is to review the dynamics that can occur, in particular, show the progression of dynamical behaviors with increasing injection intensity. Additionally, this exercise provides a bird's eye view of injection effects that will be useful for the latter discussions on noise effects. It does this by using bifurcation analysis and continuation techniques [13, 20] that are applicable only when the noise sources in Eq. (1) are neglected [19]. The results are bifurcation diagrams that map regions of distinctly different dynamical behaviors onto multidimensional spaces defined by system parameters. Figure 2 shows a bifurcation map (or diagram) useful for presenting optical injection effects. The mapping is onto a two-dimensional plane formed by injection intensity and detuning between external-signal and free-running lasers. Bifurcation curves separate regions of continuous-wave (cw), oscillatory and chaotic behaviors. The calculation is performed for a semiconductor laser described by Table I, in particular, with linewidth enhancement factor, $\alpha = 4$, which is within the range expected for bulk or quantum-well active regions. Stable time-independent solutions correspond to phase locking of the laser field to the injected field. They occupy the shaded region bounded by saddle-node S and Hopf H bifurcation curves, that become tangent at the saddle-node-Hopf point G. Outside the shaded region are solutions corresponding to orbits by the complex electric field vector of various periods, quasiperiodic tori, and chaotic attractors, all of which describe time-dependent intensities. For non-zero detuning, the system starts out with periodic oscillation for small injection intensity and progresses through a number of instabilities and complicated nonlinear dynamics

#107230 - $15.00 USD Received 3 Mar 2009; revised 27 Mar 2009; accepted 6 Apr 2009; published 22 Apr 2009

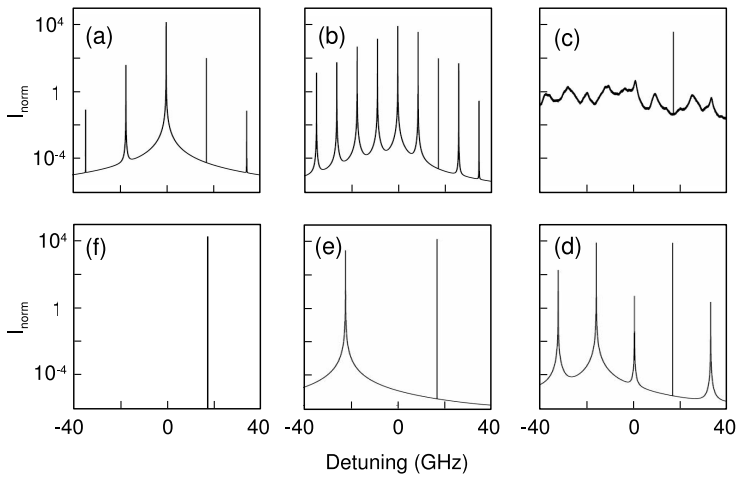

Fig. 4. Reference laser spectra for noise-free case and increasing (clockwise direction) injected intensities, (a) 0.015, (b) 0.25, (c) 0.6, (d) 18, (e) 50 and (f) 130 W/cm^2; $\Lambda = 4$ and $\Delta = 17$ GHz.

with increasing injection intensity, until locking is reached at either the Hopf bifurcation H or saddle-node bifurcation S (see, e.g., dashed line in Fig. 2). For clarity, the diagram shows only one type of bifurcation of periodic orbits namely the period-doubling (PD) bifurcation [12], identifying a typical instability involving periodic orbit of basic period.

Bifurcation diagrams can vary considerably with laser configuration. When the calculations were performed for $\alpha = 0$, a value expected for quantum dots, we found a drastic decrease in instabilities, indicating the unsuitability of a quantum-dot laser for implementing our scheme. Other factors can also influence the bifurcation curves. For example, an order of magnitude decrease in cavity decay rate increases the external-signal intensity necessary for triggering instabilities by six orders of magnitude. Additionally, the regions of complicated dynamics are appreciably smaller, and there are fewer instabilities and no chaotic dynamics.

To obtain a more visual description of changes in dynamics when crossing bifurcation boundaries, we look at the temporal and spectral behaviors of the intracavity intensity along the slice of the bifurcation diagram located by the dashed line in Fig. 2. Figure 3 shows the maxima of the time varying laser intensity versus injection intensity. (For instances when the actual value of intensity is unimportant, e.g. y-axis in Fig. 3, we find it convenient to refer to a normalized intensity defined as $I_{norm} \equiv \gamma_E \varepsilon_0 \varepsilon_b E^2/(2\hbar\nu\Gamma\gamma_N N_{th})$.) The figure shows that the laser undergoes several instabilities, displaying a rich range of complicated and chaotic oscillations. There is period-doubling bifurcation as indicated by the splitting of the single-maximum curve into two curves. Subsequent splittings with further increase in injection signal correspond to period-doubling cascade, eventually leading to complicated and chaotic oscillations that are separated by windows of periodic dynamics. The plot shows that only a small injection intensity (~ 300 mW/cm^2) is necessary for inducing the change from stable operation to complicated dynamics involving strong intensity oscillations. Note also that further increasing the injection intensity reverses the trend, with the complicated oscillations becoming period-two oscillations (double curves), then period-one oscillation (single curve), and eventually, stationary behavior, i.e., phase locked operation.

Figure 4 depicts the transitions spectrally. For injection intensities below the instability threshold the intensity spectrum consists of the free-running-laser peak (modified by the injec-

#107230 - $15.00 USD Received 3 Mar 2009; revised 27 Mar 2009; accepted 6 Apr 2009; published 22 Apr 2009

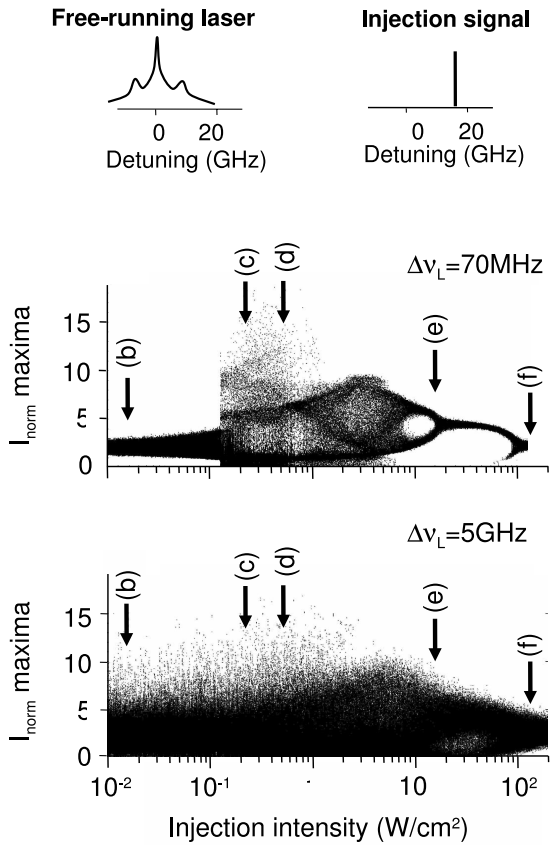

Fig. 5. Intensity maxima versus injected intensity for noise-free injection and noisy reference-laser (see top sketch); $\Lambda = 4$ and $\Delta = 17$ GHz. The reference-laser linewidths are 70MHz and 5GHz. The arrows indicate the injected intensities for the spectra in Fig. 6.

tion field via frequency pulling), a peak from the injected field (an order of magnitude smaller in intensity and detuned by Δ), and a peak at $-\Delta$ that is due to four-wave mixing of free-running and injection fields. This is shown in Fig. 4(a), which is the spectrum at injection intensity indicated by arrow (a) in Fig. 3. Just past the period doubling bifurcation [arrow (b) in Fig. 3] the spectrum contains additional peaks halfway between the original ones, as illustrated in Fig. 4(b). Further increase in injection intensity gives rise to more bifurcations leading to chaotic dynamics which manifests as a continuum of frequencies with no distinct spectral components, except for that of the injected field [Fig. 4(c)]. Then the progression inverts, signaling the onset of injection locking. The spectra corresponding to injection intensities indicated by arrows (d) to (f) are shown in Figs. 4 (d) to 4(f). They illustrate the inverse period-doubling bifurcations that finally result in phase locking via Hopf bifurcation.

Our proposal involves using the abruptness of the dynamical transitions to signal the appearance of an external laser field with sufficiently high intensity to be of concern. Take for example the stable to chaos transition. The distinct differences between the spectra depicted in Figs 4(b) and 4 (c) gives unambiguous indication of the presence of an external laser field with intensity greater than 0.1W/cm^2.

#107230 - $15.00 USD Received 3 Mar 2009; revised 27 Mar 2009; accepted 6 Apr 2009; published 22 Apr 2009

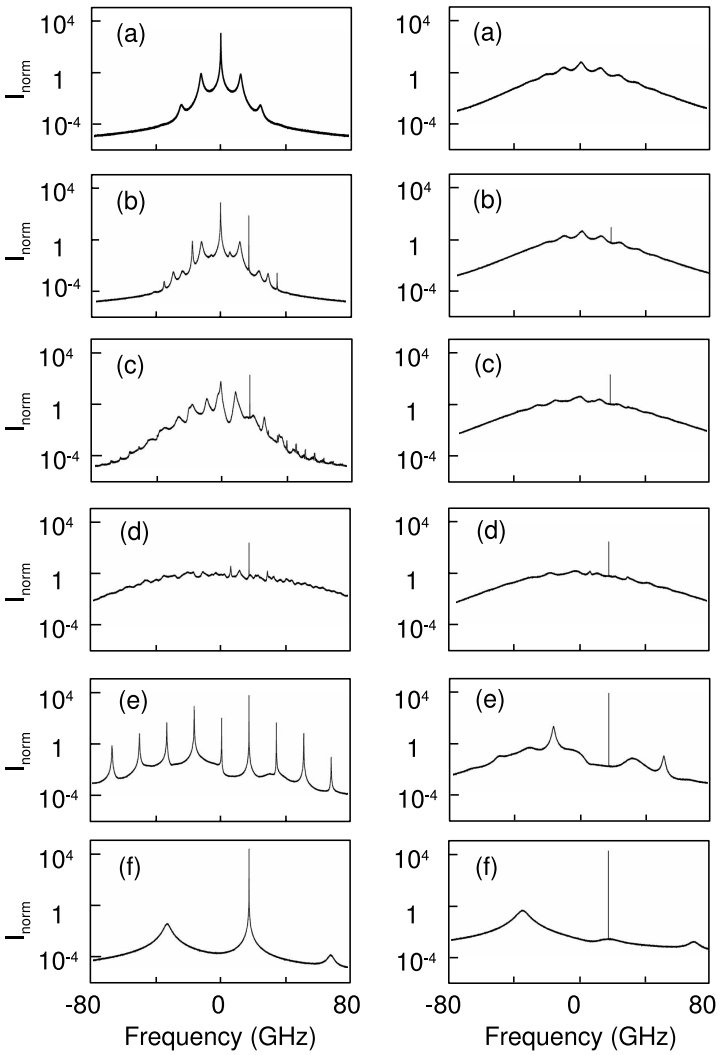

Fig. 6. Intensity spectra for reference laser linewidths of 70MHz and 5 GHz (left and right columns, respectively); $\Lambda = 4$ and $\Delta = 17$ GHz. The injected intensities are (a) 0, (b) 0.015, (c) 0.25, (d) 0.6, (e) 18 and (f) 130 W/cm^2.

3. Laser noise effects on system performance

This section exams the effects of laser noise on detector performance, in particular, the extent the bifurcation boundaries are preserved in the presence of laser field fluctuations. These fluctuations arise from spontaneous emission and changing cavity optical path length from, e.g., mechanical or temperature disturbances. Simulations are performed for a laser described by Table I and operating at three times above threshold. The noise is introduced via $F_L(t)$ with resulting reference laser linewidths of 70MHz and 5GHz, respectively. These linewidths are achievable with edge-emitting or vertical-cavity lasers and without active stabilization. The trajectory of a noisy laser was advanced with a timestep $\Delta t = 0.0005/\gamma_N$ using the Runge-Kutta fourth-order routine for the deterministic calculations involving Eqs. (1) and (2) and the Euler routine for the stochastic calculations involving Eqs. (1), (2), and (6). Following such a proce-

#107230 - $15.00 USD Received 3 Mar 2009; revised 27 Mar 2009; accepted 6 Apr 2009; published 22 Apr 2009

dure is particularly important to achieve convergence of the deterministic part for the weakly stable laser. The obtained time series of the complex laser signal were input into a Fast Fourier Transform (FFT) routine. The frequency spectra were calculated as a squared modulus of the FFT output. An individual spectrum panel in Figs. 4, 6, 8, and 9 represents the average over 500 spectra and has a resolution of $\sim$ 4MHz.

Our simulations indicate that when the laser linewidth remains narrower than its relaxation oscillation frequency, the laser field will be able to adiabatically follow the fluctuations in $F_L(t)$. In the case of an intensity maxima plot, the net result is a smearing of the intensity traces but with all bifurcations clearly distinguishable as in the noiseless situation. For the reference laser configuration considered, this is the case for laser linewidths up to approximately 10MHz. As the laser linewidth increases, the interplay of noise and injection-induced dynamics becomes stronger, resulting in certain bifurcations being unidentifiable in an intensity maxima plot. This is the case for the 70MHz laser, where the intensity maxima trace (Fig. 5, top plot) shows no indication of period-doubling bifurcations at low injection intensity. However, some features of noiseless injection-induced response remain, such as the large-amplitude oscillations and the inverse-period-doubling bifurcations leading to injection locking. These bifurcations also eventually disappear with further increase in reference-laser noise, as illustrated in the bottom intensity maxima trace for the 5GHz laser.

As discussed in the previous section, injection-induced bifurcations also appear in the form of qualitative spectral changes. In the following discussions, both in the rest of this section and the next section, we will show that in the presence of noise, these changes in intensity spectra prove to be more effective in uncovering bifurcations. The results are presented in two columns in Fig. 6 (left and right columns for 70MHz and 5GHz linewidths, respectively). Successive rows illustrate the progression of spectral behavior with increasing injection intensity, starting with the free-running (i.e., zero injection intensity) spectra in the top row. Here, the 70MHz spectrum contains relaxation oscillation created by the temporal fluctuations in $F_L(t)$. The resonances are at $\pm$12GHz and higher harmonics, These resonances eventually blend into the background as shown in the 5GHz spectrum.

The remaining rows in Fig. 6 are for non-zero injection intensities, with values given in the figure caption and indicated by arrows in the intensity maxima plots in Fig. 5. First, we concentrate on the stable to chaos transition at weak injection intensity. In contrast to the intensity maxima plot (Fig. 5, top trace), we see the full progression of bifurcations, from basically free-running (with the exception of 4-wave mixing between free-running and injection fields) to period-doubling and then to chaos, for the 70MHz linewidth (left column). The corresponding spectra for the 5GHz laser indicate greater difficulty in identifying the low injection intensity bifurcations (right column), because of the difficulty in distinguishing between broadband reference laser operation and chaos, given a finite measurement bandwidth. However, the transitions from chaos or broadband operation to stable or injection-locked operation are identifiable for both laser linewidths, even though the intermediate invert-period-doubling stage is somewhat ambiguous for the 5GHz case. Reference laser operation with a sharp injection signal resonance, together with suppression of noise (by over 2 orders of magnitude as seen by comparing noise levels in rows c and e) is always achievable via injection locking. Of course, higher injection intensity is necessary with higher reference laser noise.

In terms of remote sensing of laser radiation using our scheme, the results indicate an upper limit in the reference laser linewidth for using the stable to chaos transition, which has the advantage of occurring at very low injection intensity. On the other hand, if practical constraints prevents reference laser design for, say less than 100MHz linewidth operation, then the chaos to injection-locked transition provides an alternative for implementing our scheme. The disadvantage, compared to the stable to chaos transition, is less sensitivity to weak external signals.

#107230 - $15.00 USD Received 3 Mar 2009; revised 27 Mar 2009; accepted 6 Apr 2009; published 22 Apr 2009

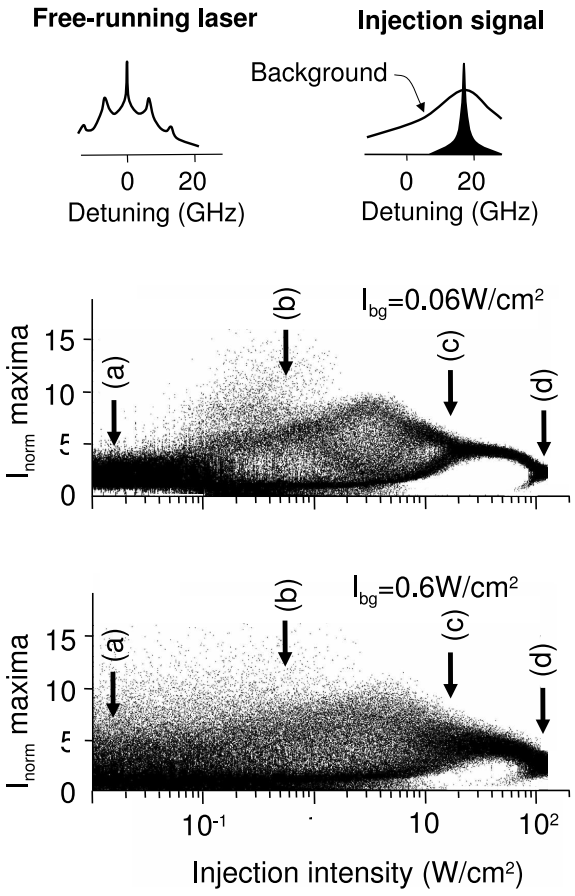

Fig. 7. Intensity maxima versus coherent injected intensity for 70MHz reference laser and injected signal (see top sketch); $\Lambda = 4$ and $\Delta = 17$ GHz. The incoherent injected contributions are 0.06 and 0.6W/cm^2. The arrows indicate the coherent injected intensities for the spectra in Figs. 8 and 9.

4. Effects of noise presence in injection signal

This section exams the effects of noise in the injected signal, by considering an injected signal consisting of coherent and incoherent contributions. The coherent contribution is from the laser whose presence we wish to detect, while the incoherent contribution comes from, e.g., thermal emission from the earth's surface. So far, we have seen that bifurcations can be generated by a very small coherent injection. This turns out not to be the case when the injection is totally incoherent. During simulations, we have encountered situations where it is impossible to produce a noticeable stable to chaos transition with incoherent injection, even with four orders of magnitude higher intensity than that necessary with coherent injection. This may imply that when both coherent and incoherent contributions are present, the coherent intensity has to exceed the incoherent one to produce any bifurcation that is useful to our scheme. If that is the case, an important question is the extend the coherent contribution has to exceed the incoherent one before it can be detected via bifurcations.

In the following discussion, we use an injected signal whose spectrum consists of a narrow (coherent) resonance superimposed upon a broad (incoherent) background. We choose the ran-

#107230 - $15.00 USD Received 3 Mar 2009; revised 27 Mar 2009; accepted 6 Apr 2009; published 22 Apr 2009

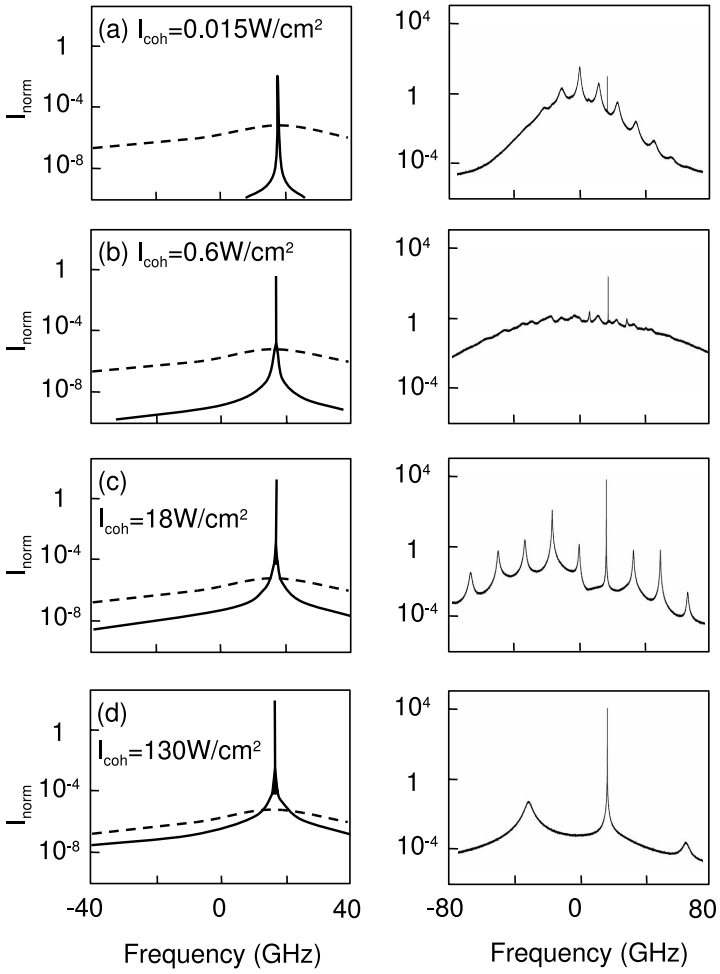

Fig. 8. Spectral response for 70MHz reference laser and low incoherent injection ; $\Lambda = 4$ and $\Delta = 17$ GHz.(Left column) Injected intensity spectra with solid and dashed curves showing coherent and incoherent contributions, respectively. From top to bottom, the coherent contributions are (a) 0.015, (b) 0.6, (c) 18 and (d) 130W/cm^2, while the incoherent contribution is clamped at 0.06W/cm^2. (Right column) Corresponding reference-laser intensity spectra.

dom noise functions giving rise to injected and reference laser noise so that the coherent and incoherent injected contributions have linewidths of 1MHz and 20GHz, respectively, and the reference laser linewidth is 70MHz [see Fig. 6(a, left) for the free-running laser spectrum]. Figure 7 shows the intensity maxima plots versus injected laser intensity for two background levels. The plots show that for the chosen reference laser configuration, somewhere between 0.01W/cm^2 and 0.1W/cm^2 is the injected noise level above which the low injection bifurcations become unobservable. For low injected laser intensities, both plots show a wide and uniform spread of maxima values, arising from the strong response of the reference laser to the injected noise. For the lower background level of 0.06W/cm^2, the increase in intensity maxima spread around an injected laser intensity of 0.2W/cm^2, suggests the presence of a stable to chaos transition. At high injection intensity, the intensity maxima spread narrows, indicating stabilization

#107230 - $15.00 USD Received 3 Mar 2009; revised 27 Mar 2009; accepted 6 Apr 2009; published 22 Apr 2009

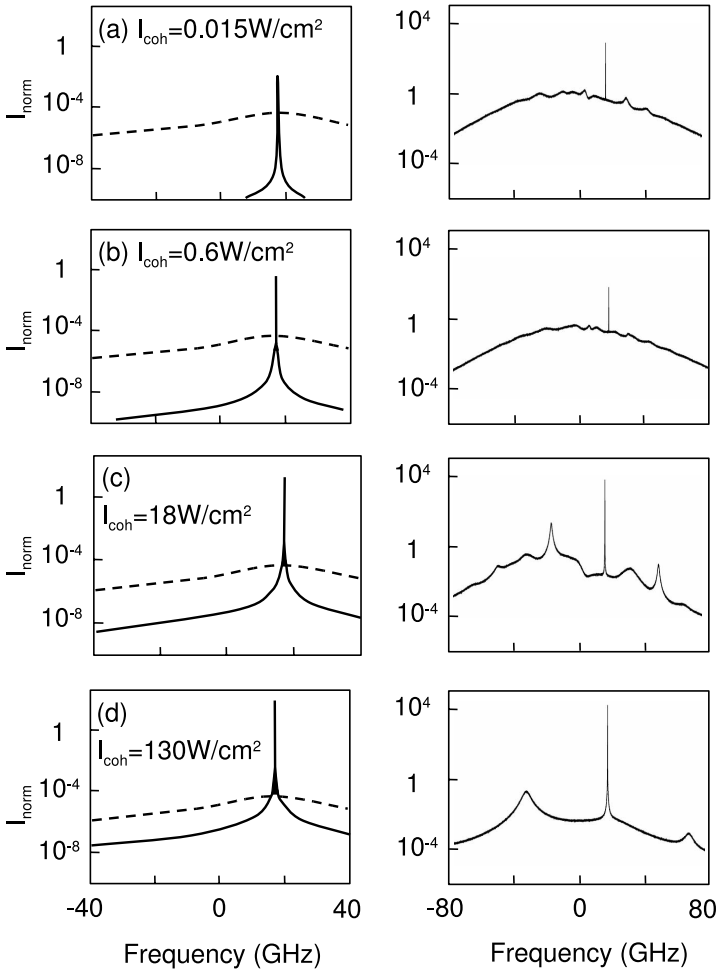

Fig. 9. Spectral response for 70MHz reference laser and high incoherent injection; $\Lambda = 4$ and $\Delta = 17$ GHz. (Left column) Injected intensity spectra with solid and dashed curves showing coherent and incoherent contributions, respectively. From top to bottom, the coherent contributions are (a) 0.015, (b) 0.6, (c) 18 and (d) 130W/cm^2, while the incoherent contribution is clamped at 0.6W/cm^2. (Right column) Corresponding reference-laser intensity spectra.

of the reference laser via injection locking. There is even a faint indication of inverse period doubling for the low injected noise case. Even so, the overall lack of abrupt changes at both background noise levels makes difficult the use of intensity maxima for estimating the locations of bifurcation boundaries.

In contrast, the spectra in Figs. 8 and 9 provide a more encouraging picture of the viability of our scheme for discriminating the laser signal from the noisy background. The figures illustrate the spectral changes with increasing injected laser intensity for the two background levels considered in the previous paragraph. Each figure shows the injected signal and reference laser spectra in the left and right columns, respectively. The rows are for the injected laser intensities indicated by arrows in the intensity maxima plots in Fig. 7. With a weak background, one can see a vague but usable transition from free-running to chaos operation [Figs. 8 (a) with the

#107230 - $15.00 USD Received 3 Mar 2009; revised 27 Mar 2009; accepted 6 Apr 2009; published 22 Apr 2009

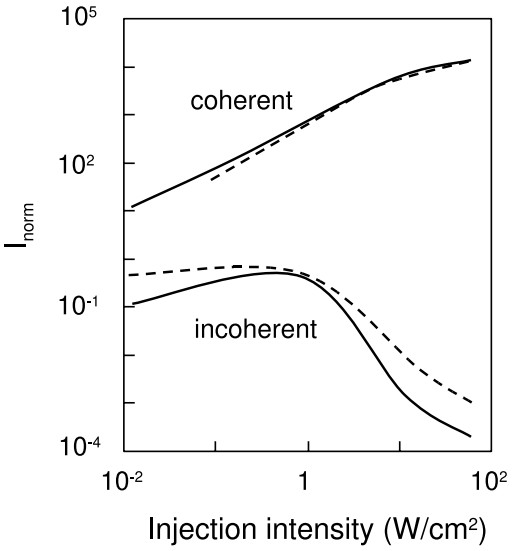

Fig. 10. Coherent and incoherent normalized peak intensities in reference laser versus injected coherent intensity for background noise of 0.06W/cm^2 (solid curve) and 0.6W/cm^2 (dashed curve).

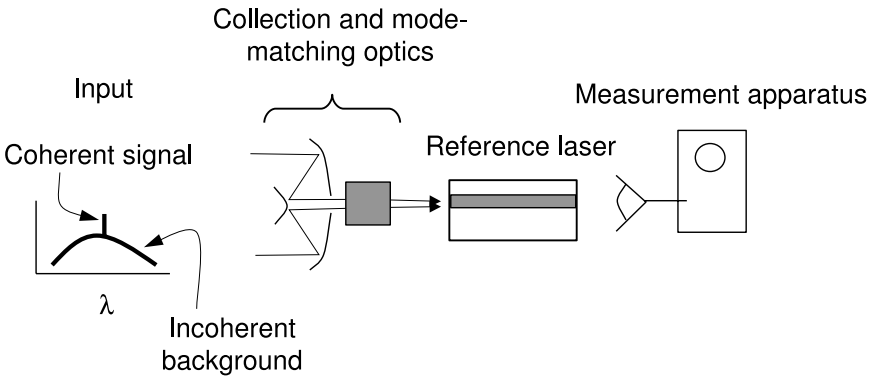

Fig. 11. Experimental setup for a remote laser radiation sensor with basic components: (a) light collection optics, (b) reference laser and (c) detection scheme for bifurcations.

relaxation oscillation resonances and 8(b) with a basically featureless spectrum]. More unambiguous are the chaos to inverse period doubling to injection locked bifurcations [Figs. 8(b) to (d)]. With the strong noise background (Fig, 9), while there is basically no difference between the top two spectra, the transitions from chaos or broadband to injection-locked operation (bottom 3 spectra) are clearly present. Also interesting, because its presence is not indicated in the intensity maxima plot, is that occurrence of inverse period doubling, which reinforces our claim that spectral change is a more sensitive detection method of bifurcation occurrences.

Figures 8 and 9 show that with both noise backgrounds, there is a suppression of intracavity noise level as injection locking comes into play. A clearer indication is obtained from Fig. 10 where we plotted both the intracavity coherent and incoherent intensities as a function of injected coherent intensity. The values are obtained from spectra including those shown in Figs.

#107230 - $15.00 USD Received 3 Mar 2009; revised 27 Mar 2009; accepted 6 Apr 2009; published 22 Apr 2009

8 and 9. The coherent contribution is the peak intensity at the injection frequency. The incoherent contribution, we take to be the maximum intensity of the broad background. The curves for the coherent contribution show that the noise background does not affect the amplification of the coherent injected signal. Both curves increases linearly with injected intensity for small injection intensity and then saturates at high injection intensity, consistent with a homogeneously broadened gain medium. For the incoherent contribution, the figure shows three orders of magnitude suppression of noise with injection locking, with the onset of noise suppression occurring while the coherent contribution is still growing strongly. This strong filtering of the noise by the active optical cavity translates to significant improvement in signal to noise ratio from injection locking.

5. Conclusion

This paper describes a solution to the problem of detecting weak laser radiation in the presence of a strong incoherent background. The method is based on the extreme sensitivity of laser dynamical nonlinearities to an injected signal, which leads to bifurcations, e.g., sharp transitions between stable and chaotic states of laser operation. Our proposal is to use the occurrences of such bifurcations as warning of irradiation by a laser source A possible experimental arrangement is illustrated in Fig. 11. The basic components are the light collection optics, reference laser and bifurcation detection scheme. The collection optics may be a telescope or a tapered fiber bundle for mode matching into reference laser waveguide. Numerical simulations suggest a semiconductor quantum-well laser operating with a microcavity, e.g., a vertical-cavity surface-emitting laser (VCSEL) as a good choice for the reference laser. Detection of bifurcations may be via changes in spectrum or intensity fluctuations. As discussed in this paper, spectral changes are more sensitive to bifurcation occurrences in the present of noise. Using such a baseline scheme, our simulations demonstrated significant qualitative and quantitative differences in the response of the reference laser to the intensity and coherence of the injected signal. There is also considerable modification of bifurcation boundaries by changing active medium and optical resonator configurations. We encountered situations where bifurcations can be induced with a coherent injected intensity that is over six orders of magnitude smaller than the reference laser's intracavity intensity. Discrimination between coherent and incoherent injection also looks promising because of the over three orders of magnitude background noise suppression with injection locking.

Acknowledgments

The work is supported by the United States Department of Energy's Laboratory Directed Research and Development (LDRD) program at Sandia National Laboratories and by the Alexander von Humboldt Foundation.

#107230 - $15.00 USD Received 3 Mar 2009; revised 27 Mar 2009; accepted 6 Apr 2009; published 22 Apr 2009